

ChemComm

Accepted Manuscript



This article can be cited before page numbers have been issued, to do this please use: Y. Kikkawa, M. Nagasaki, E. Koyama, S. Tsuzuki and K. Hiratani, *Chem. Commun.*, 2019, DOI: 10.1039/C9CC00532C.



This is an Accepted Manuscript, which has been through the Royal Society of Chemistry peer review process and has been accepted for publication.

Accepted Manuscripts are published online shortly after acceptance, before technical editing, formatting and proof reading. Using this free service, authors can make their results available to the community, in citable form, before we publish the edited article. We will replace this Accepted Manuscript with the edited and formatted Advance Article as soon as it is available.

You can find more information about Accepted Manuscripts in the [author guidelines](#).

Please note that technical editing may introduce minor changes to the text and/or graphics, which may alter content. The journal's standard [Terms & Conditions](#) and the ethical guidelines, outlined in our [author and reviewer resource centre](#), still apply. In no event shall the Royal Society of Chemistry be held responsible for any errors or omissions in this Accepted Manuscript or any consequences arising from the use of any information it contains.

Hexagonal array formation by intermolecular halogen bonding using a binary blend of linear building blocks: STM study

Yoshihiro Kikkawa,* Mayumi Nagasaki, Emiko Koyama, Seiji Tsuzuki and Kazuhisa Hiratani

Received 00th January 20xx,
Accepted 00th January 20xx

DOI: 10.1039/x0xx00000x

www.rsc.org/

Hexagonal arrays were fabricated via intermolecular halogen bonding between two linear molecular building blocks in a bicomponent blend. The substitution position of the pyridine N atom involved in the halogen bond plays an important role in the formation of the hexagonal structures.

Halogen bonds, which form between electrophilic halogen atoms and nucleophilic atoms such as those with lone pairs, are highly directional interactions with strengths comparable to those of hydrogen bonds.¹ Halogen bonds are generally described as R-X...Y, where X is a halogen atom covalently linked to the R group, the three dots represent the halogen bond, and Y is the halogen bond acceptor. The magnitude of the halogen bond is mainly controlled by the electrostatic interaction of the halogen atom, and follows the order Cl < Br < I.² Halogen bonds are known to play important roles in the formation of supramolecular structures in artificial and biological systems.³

The formation of hexagonal arrays on a solid substrate has been achieved using C₃-symmetric molecular building blocks with rigid molecular frameworks, and their structures have been revealed using scanning tunnelling microscopy (STM) at molecular resolution.⁴ The hexagonal spaces have been utilized as templates to accommodate guest molecules.⁵ De Feyter and Tobe et al. prepared rigid and C₃-symmetric dihydrobenzo[12]annulenes to construct porous hexagonal networks through the interdigitation of the alkyl chains, and studied the formation of the hexagonal structures, pore size tuning, chiral assemblies, and guest incorporation into the hexagonal pores for host-guest chemistry.⁶

The construction of molecular assemblies through halogen bonding has attracted increasing attention.⁷ For example, Wan et al. demonstrated the formation of 2D hexagonal porous

networks using a binary blend of 1,3,5-tris(ethynylpyridyl)benzene and 1,3,5-trifluoro-2,4,6-triiodobenzene; they emphasized that electrical stimulus was important to induce the formation of the 2D networks via halogen bonding.^{7k} However, to the best of our knowledge, there have been no reports of the formation of honeycomb structures through halogen bonding using a bicomponent blend of linear building blocks without C₃ symmetry.

In this contribution, we prepared compounds **1** and **2**, which contain lone pairs and halogen atoms as halogen bonding sites, respectively (Chart 1). The compounds **p1** and **m1**, which varied only in the pyridine substitution position, were prepared to study the effect of the substitution position on the formation of the 2D structure via halogen bonding. The 2D structure of each component was studied using STM at the highly oriented pyrolytic graphite (HOPG)/1-phenyloctane interface. Then, the STM observations were performed for bicomponent blends of **m1** and **p1** with **2** (1:1 ratio). In addition, the intermolecular interactions between **1** and **2** were studied through DFT calculations using the program Gaussian 09.⁸

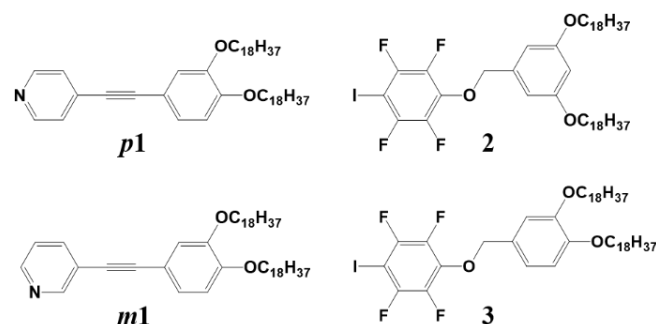


Chart 1 Chemical structures of compounds **1**, **2**, and **3** prepared in this study.

National Institute of Advanced Industrial Science and Technology (AIST), Tsukuba Central 5, 1-1-1 Higashi, Tsukuba, Ibaraki 305-8565, Japan

Electronic Supplementary Information (ESI) available: Experimental detail, additional STM images, lattice constants, molecular models, and statistical analysis of 2D structure formation. See DOI: 10.1039/x0xx00000x

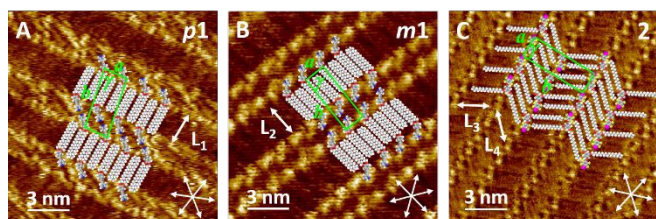


Fig. 1 STM images of **p1**, **m1** and **2** (1 mM) physisorbed at the HOPG/1-phenyloctane interface. Molecular models are superimposed on the STM images. A set of arrows indicates the HOPG lattice directions. Tunnelling conditions: (A) $I = 1.3$ pA, $V = -566$ mV, (B) $I = 2.0$ pA, $V = -390$ mV, (C) $I = 1.0$ pA, $V = -566$ mV.

First, the 2D structures of the mono-component systems were observed using STM at the HOPG/1-phenyloctane interface. Fig. 1A shows the STM image of **p1**, which formed columns consisting of two parallel bright lines that were sandwiched between dark troughs with a width L_1 of 2.07 ± 0.13 nm. The L_1 value was identical to the length of the octadecyl chain (2.16 nm; Fig. 1A). The bright and dark contrast areas corresponded to the π -conjugated motif and octadecyl chains in **p1**, respectively. A molecular model was developed, and is superimposed on the STM image. The para-substituted pyridine moieties were oriented in a face-to-face manner, and the alkyl chain pairs of the molecules were arranged side-by-side; neighbouring molecules were orientated in opposite directions. The lattice constants of the 2D structures are summarized in Table S1 (ESI).

A similar 2D structure was found for **m1**; namely, a double columnar structure was formed, as shown in Fig. 1B. The alternating arrangement of the neighbouring alkyl chain units ($L_2 = 2.06 \pm 0.20$ nm) was also found in the physisorbed **m1** monolayer. From Fig. 1A and 1B, it can be concluded that the substitution position of pyridine in **1** does not significantly influence 2D structure formation, as **p1** and **m1** formed nearly identical 2D structures.

A single-line columnar structure was observed for **2**, and is shown in Fig. 1C. The 3,5-alkyloxy chains of each molecule were not parallel to one another, but instead assumed an expanded conformation with an angle of $119 \pm 6^\circ$ to maximize the dispersion forces between neighbouring molecules. The alkyl chains thus formed a herringbone structure with lengths of $L_3 = 2.21 \pm 0.14$ nm and $L_4 = 2.33 \pm 0.19$ nm, and the direction of the iodine atom of **2** alternated in adjacent columns. It is noteworthy that the 2D structures of **p1**, **m1**, and **2** were not affected by the concentration of the 1-phenyloctane solution within the range of $62.5 \mu\text{M}$ – 2 mM, *i.e.* there was no concentration effect on the 2D structure in these mono-component systems.

After study of the mono-component systems, binary blends were prepared, expecting I...N halogen bonding,³ which produced supramolecular 2D assemblies that were different from those of **1** and **2**. The effect of the pyridine substitution position on the 2D structure formation was examined using bicomponent blends of **m1** and **p1** with **2**.

Fig. 2 shows the STM image of the bicomponent blend of **p1** and **2** (0.125 mM) observed at the HOPG/1-phenyloctane interface.⁹ Parallel linear columns with bright contrast were

separated by regular dark troughs, which were attributed to the alkyl chain units ($L_5 = 2.07 \pm 0.22$ nm, Fig. 2A). The bright columns were composed of short stick-like parallel structures. Taking the I...N halogen bond into account, the short sticks were attributed to the π -conjugated unit of **p1** and the two aromatic rings of **2**, one of which was functionalized with halogens while the other possessed alkyloxy chains (Fig. S2, ESI). DFT calculations (Fig. S3, ESI) suggested that pairs of **p1** and **2** molecules were arranged periodically, with neighbouring **p1/2** pairs having opposite orientations due to Ar-F...H-Py interactions between neighbouring pairs in addition to the halogen bond within each pair. The proposed molecular model is shown in Fig. 2B. Due to the close packing of the bright stick-like structures comprising the columns, there was not enough space for all the alkyl chains to be accommodated in the lattice. Thus, only one of the two alkyloxy chains of each **p1** and **2** unit was attached to the HOPG surface; the other alkyl chain was not adsorbed on the substrate, but instead was directed towards the solvent phase.

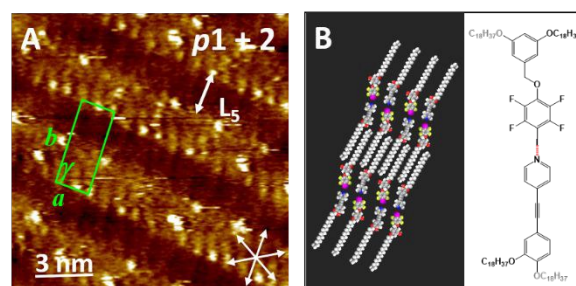


Fig. 2 STM image of the bicomponent blend of **p1** and **2** observed at the HOPG/1-phenyloctane interface (A). A set of arrows indicates the HOPG lattice directions. Panel (B) shows the proposed molecular model based on the STM images and DFT calculation (Fig. S3, ESI) and the geometry of the I...N halogen bond. Tunnelling conditions: $I = 1.3$ pA, $V = -800$ mV.

Of particular interest is the formation of hexagonal arrays by the bicomponent blend of **m1** and **2** (1 mM), shown in Fig. 3A. The *m*-substitution of the **m1** pyridine allowed the arrangement of the **2** units at an angle of ca. 120° via the I...N halogen bonding (Fig. 3B). The halogen bonds and the Ar-F...H-Py interactions among three pairs of **2** and **m1** molecules (Fig. S4, ESI) formed triangular helical assemblies; the alkyl chains of these assemblies associated to surround hexagonal pores ($L_6 = L_7 = 2.16 \pm 0.19$ nm). In the proposed model shown in Fig. 3B, the alkyl chains of **m1** were aligned parallel to one another, whereas those of **2** were expanded, as evidenced by the highly resolved STM images in Figs. 3C, 3D, and S5 (ESI). It is noteworthy that the binary blend of **m1** and compound **3**,¹⁰ which was the 3,4-alkyloxy substituted analogue of **2**, did not show a hexagonal structure, but instead displayed only the double columnar structure originating from **m1** under the present experimental conditions. This result suggests that the 3,5-dialkyloxy substitution in **2** is indispensable for the formation of a hexagonal structure in the present bicomponent blend system, possibly due to the preorganization of the alkyl chains along the two sides of a hexagonal framework.

Several groups have reported that 2D chirality can be introduced and expressed by even achiral molecule assemblies on a surface.¹¹ Careful analysis of the STM images revealed clockwise (CW) and counter-clockwise (CCW) helical triangular structures, as shown in Fig. S7 (ESI). This result suggests that the chirality in the 2D structure was induced by the different orientations of the halogen-bonded pairs of the linear molecules **m1** and **2**. At the centre of the honeycomb structure, molecules of the solvent 1-phenyloctane may have dynamically filled the vacant space to stabilize the 2D structure.

At a concentration of 1 mM, linear structures were also observed in addition to the hexagonal ones, as shown in Fig. S8 (ESI). These linear structures corresponded to those observed for the mono-component systems of **m1** and **2**. It has been reported that the concentration of the components in the solution sometimes affects 2D structure formation at the solid/liquid interface, and that the molecular density on the surface increases with an increase in the solution concentration.¹² Thus, the effect of the concentration of the premixed solution on the 2D structure was investigated for the bicomponent blend of **m1** and **2**. Fig. S9 (ESI) shows wide-area STM images of the bicomponent blend at different concentrations. At the highest concentration, the linear structures were predominant, whereas at lower concentrations, the area of the linear structures decreased, and the population of hexagonal arrays increased. The areas of the honeycomb and linear structures at different concentrations were evaluated from ten 200 nm × 200 nm STM images, and the resulting ratios are shown in Fig. S10 (ESI). Although some areas displayed unstable structures which could not be distinguished as either hexagonal or linear domains, essentially, the lower the concentration of the solution, the larger the population of hexagonal arrays. For the lowest concentration examined (62.5 μM), hexagonal structures and unstable domains each occupied about half the surface, and the blurred contrast observed for the unstable domains may have been due to the presence of low density and unstable molecular assemblies on the HOPG surface.

In previous studies, halogen-bonded 2D networks composed of I...N interactions were prepared either by simply mixing the solutions of constituents^{7f} or by the instantaneous pulsed current applied between the substrate and the STM tip.^{7k} In our present study, the hexagonal arrays were effectively formed by adjusting the concentration of the pre-mixed solution, with greater numbers of honeycomb structures being observed on the HOPG surface at low concentrations. The molecular density of the 2D structures in **m1** and **2** was calculated from the lattice constants to be 0.32 and 0.29 molecule/nm², respectively. In contrast, the molecular density of the honeycomb structure in the bicomponent blend (**m1+2**) was 0.12 molecule/nm² (per one of the constituents). Therefore, we propose that the low concentration of the building blocks resulted in the reduced molecular density of the 2D structure on the surface, allowing the preferential formation of honeycomb structures: the triangular helical assemblies were formed at the vertices of the hexagon via both halogen bonding and Ar-F...H-Py interactions. In addition, the expanded orientation of the alkyl chains in **2** guided the arrangement of the **m1** alkyl chains to surround a hexagonal pore, resulting in the formation of supramolecular honeycomb structure frameworks on the surface.

In summary, double columnar (**p1** and **m1**) and single-line columnar structures (**2**) were observed in the mono-component systems, by using STM at the HOPG/1-phenyloctane interface. Formation of I...N halogen bonding allowed the construction of supramolecular complexes on the surface. The short and stick-like objects formed between **p1** and **2** via halogen bond aligned

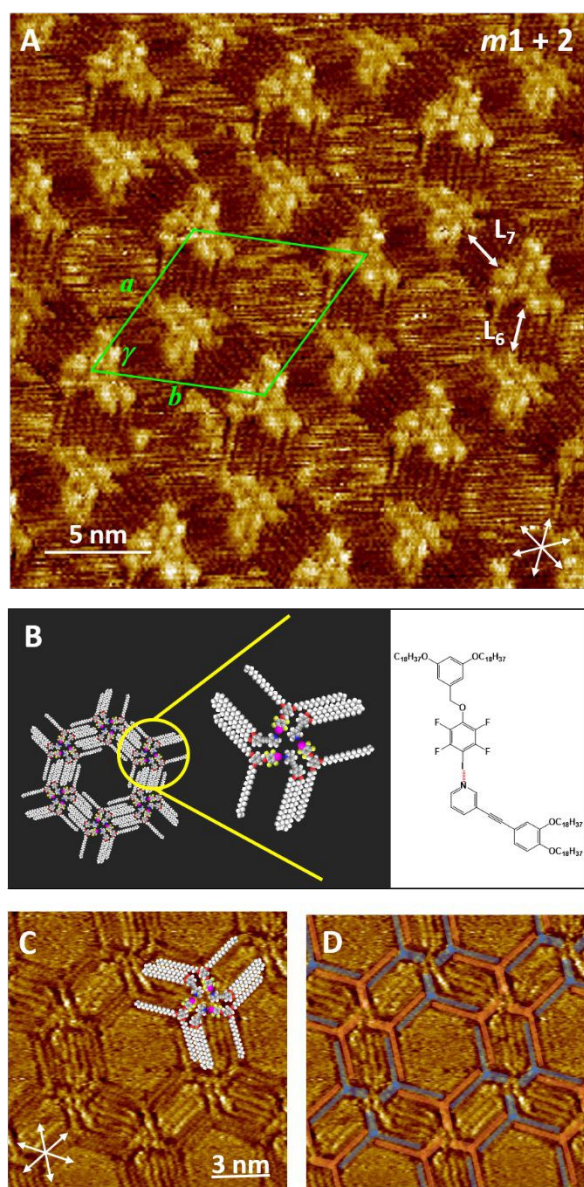


Fig. 3 (A) STM image of the bicomponent blend of **m1** and **2** (1 mM) at the HOPG/1-phenyloctane interface, and (B) the proposed molecular model based on the STM images and DFT calculation (Fig. S4, ESI). Due to the meta substitution of pyridine and the halogen bond, the angle between **m1** and **2** was ca. 120°. (C) Highly resolved STM image of the hexagonal arrays, on which the molecular model of a triangular helical assembly with alkyl chains was superimposed; in (D) the building blocks **2** are highlighted in blue and red. The expanded orientation of the alkyl chains of **2** is evident from the STM image, and the orientation of **m1** is shown in Fig. S4 (ESI). Note that panels (A, B) and (C, D) are chiral (see Fig. S7, ESI). A set of arrows indicates the HOPG lattice directions. Tunnelling conditions: (A) $I = 1.0$ pA, $V = -650$ mV, (C) $I = 2.0$ pA, $V = -353$ mV.

in a parallel fashion to create a linear structure different from those of the single component systems. Hexagonal arrays could be efficiently fabricated in the mixture of **m1** and **2**, despite the linear molecular building blocks. Cooperative I...N halogen bonding and Ar-F...H-Py interactions formed triangular helical assemblies. In addition, the preorganization of the alkyl chains in **2** assisted the orientation of those of **m1** along the hexagonal framework, resulting in the formation of fascinating honeycomb structures. Effective fabrication of the honeycomb structures was achieved by tuning the concentration of the blend solution, and lower concentrations were found to increase the area over which the hexagonal arrays were formed.

The present study provided a rational method to construct hexagonal arrays composed of a bicomponent blend of two linear molecular building blocks via intermolecular halogen bonding. We believe that supramolecular complex formation induced by the directional halogen bonding contributes to the development of molecular assembly techniques, and should be applicable to the efficient production of nano-architectures and their regular arrangement on a surface.

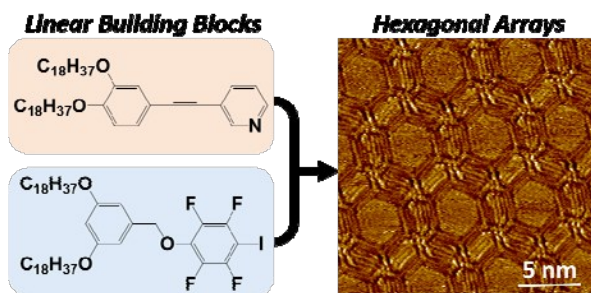
This work was partly supported by the JSPS KAKENHI (17K05851). We thank Dr. Hiroaki Sato and Dr. Thierry Fouquet for the HR-MALDI-MS analysis.

Conflicts of interest

There are no conflicts to declare.

Notes and references

- (a) G. Cavallo, P. Metrangolo, R. Milani, T. Pilati, A. Priimagi, G. Resnati and G. Terraneo, *Chem. Rev.*, 2016, **116**, 2478; (b) R. Tepper and U. S. Schubert, *Angew. Chem. Int. Ed.*, 2018, **57**, 6004.
- (a) S. Tsuzuki, A. Wakisaka, T. Ono and T. Sonoda, *Chem. Eur. J.*, 2012, **18**, 951; (b) S. Tsuzuki, T. Uchimaru, A. Wakisaka, T. Ono and T. Sonoda, *Phys. Chem. Chem. Phys.*, 2013, **15**, 6088.
- (a) E. Persch, O. Dumele and F. Diederich, *Angew. Chem. Int. Ed.*, 2015, **54**, 3290; (b) L. C. Gilday, S. W. Robinson, T. A. Barendt, M. J. Langton, B. R. Mullaney and P. D. Beer, *Chem. Rev.*, 2015, **115**, 7118.; (c) J. Poznański, M. Winiewska, H. Czapinska, A. Poznańska and D. Shugar, *Acta Biochim. Pol.*, 2016, **63**, 203; (d) B. Li, S.-Q. Zang, L.-Y. Wang and T. C. W. Mak, *Coord. Chem. Rev.*, 2016, **308**, 1.;
- (a) R. Gutzler, T. Sirtl, F. Dienstmaier, K. Mahata, W. M. Heckl, M. Schmittl and M. Lackinger, *J. Am. Chem. Soc.*, 2010, **132**, 5084; (b) T. Chen, G.-B. Pan, H. Wettach, M. Fritzsche, S. Höger, L.-J. Wan, H.-B. Yang, B. H. Northrop, and P. J. Stang, *J. Am. Chem. Soc.*, 2010, **132**, 1328; (c) D. Bléger, D. Kreher, F. Mathevet, A.-J. Attias, G. Schull, A. Huard, L. Douillard, C. Fiorini-Debuischert and F. Charra, *Angew. Chem. Int. Ed.*, 2007, **46**, 7404; (d) R. Gutzler, S. Lappe, K. Mahata, M. Schmittl, W. M. Heckl and M. Lackinger, *Chem. Commun.*, 2009, 680; (e) S. Wu, S. Xu, Y. Geng, Z. Liu, H. Nie, L. Shu, K. Deng, Q. Zeng and C. Wang, *J. Phys. Chem. C*, 2016, **120**, 12618.; (f) Z. Ma, Y.-Y. Wang, P. Wang, W. Huang, Y.-B. Li, S.-B. Lei, Y.-L. Yang, X.-L. Fan and C. Wang, *ACS Nano*, 2007, **1**, 160; (g) M. O. Blunt, J. C. Russell, M. del C. Gimenez-Lopez, N. Taleb, X. Lin, M. Schröder, N. R. Champness and P. H. Beton, *Nat. Chem.*, 2010, **3**, 74; (h) C.-A. Palma, M. Bonini, A. Llanes-Pallas, T. Breiner, M. Prato, D. Bonifazi, and P. Samori, *Chem. Commun.*, 2008, 5289.
- J. Teyssandier, S. De Feyter and K. S. Mali, *Chem. Commun.*, 2016, **52**, 11465, and the references cited therein.
- Y. Tobe, K. Tahara and S. De Feyter, *Bull. Chem. Soc. Jpn.*, 2016, **89**, 1277, and the references cited therein.
- (a) A. Vanderkooy and M. S. Taylor, *J. Am. Chem. Soc.*, 2015, **137**, 5080; (b) H. L. Nguyen, P. N. Horton, M. B. Hursthouse, A. C. Legon and D. W. Bruce, *J. Am. Chem. Soc.*, 2004, **126**, 16; (c) M. Kondo, K. Okuomoto, S. Miura, T. Nakanishi, J. Nishida, T. Kawase and N. Kawatsuki, *Chem. Lett.*, 2017, **46**, 1179; (d) F. Wang, N. Ma, Q. Chen, W. Wang and L. Wang, *Langmuir*, 2007, **23**, 9540; (e) F. Silly, *J. Phys. Chem. C*, 2013, **117**, 20244; (f) A. Mukherjee, J. Teyssandier, G. Hennrich, S. De Feyter and K. S. Mali, *Chem. Sci.*, 2017, **8**, 3759; (g) Z. Guo, P. Yu, K. Sun, S. Lei, Y. Yi and Z. Li, *Phys. Chem. Chem. Phys.*, 2017, **19**, 31540; (h) B. Zha, X. Miao, P. Liu, Y. Wu and W. Deng, *Chem. Commun.*, 2014, **50**, 9003; (i) Y. Makoudi, M. Beyer, J. Jeannoutot, F. Picaud, F. Palmino and F. Chérioux, *Chem. Commun.*, 2014, **50**, 5714; (j) D. Peyrot and F. Silly, *ACS Nano*, 2016, **10**, 5490; (k) Q.-N. Zheng, X.-H. Liu, T. Chen, H.-J. Yan, T. Cook, D. Wang, P. J. Stang and L.-J. Wan, *J. Am. Chem. Soc.*, 2015, **137**, 6128.
- (a) Gaussian 09, Revision C01, M. J. Frisch, G. W. Trucks, H. B. Schlegel, G. E. Scuseria, M. A. Robb, J. R. Cheeseman, G. Scalmani, V. Barone, B. Mennucci, G. A. Petersson, H. Nakatsuji, M. Caricato, X. Li, H. P. Hratchian, A. F. Izmaylov, J. Bloino, G. Zheng, J. L. Sonnenberg, M. Hada, M. Ehara, K. Toyota, R. Fukuda, J. Hasegawa, M. Ishida, T. Nakajima, Y. Honda, O. Kitao, H. Nakai, T. Vreven, J. A. Montgomery Jr., J. E. Peralta, F. Ogliaro, M. Bearpark, J. J. Heyd, E. Brothers, K. N. Kudin, V. N. Staroverov, R. Kobayashi, J. Normand, K. Raghavachari, A. Rendell, J. C. Burant, S. S. Iyengar, J. Tomasi, M. Cossi, N. Rega, J. M. Millam, M. Klene, J. E. Knox, J. B. Cross, V. Bakken, C. Adamo, J. Jaramillo, R. Gomperts, R. E. Stratmann, O. Yazyev, A. J. Austin, R. Cammi, C. Pomelli, J. W. Ochterski, R. L. Martin, K. Morokuma, V. G. Zakrzewski, G. A. Voth, P. Salvador, J. J. Dannenberg, S. Dapprich, A. D. Daniels, Ö. Farkas, J. B. Foresman, J. V. Ortiz, J. Cioslowski, and D. J. Fox, Gaussian, Inc., Wallingford CT, 2009; (b) Details of the computational methods are provided in the ESI.
- It was difficult to obtain clear STM images at concentrations higher than 0.125 mM. In some cases, double columnar structures possibly composed of **p1** were found as separated domains, in addition to the major 2D structure in Fig. 2, as shown in Fig. S1 (ESI).
- The compound **3** could form the self-assembled 2D structure, as shown in Fig. S6 (ESI).
- (a) N. Katsonis, H. Xu, R. M. Haak, T. Kudernac, Ž. Tomović, S. George, M. Van der Auweraer, A. P. H. J. Schenning, E. W. Meijer, B. L. Feringa and S. De Feyter, *Angew. Chem. Int. Ed.*, 2008, **47**, 4997; (b) S. Lei, M. Surin, K. Tahara, J. Adisojoso, R. Lazzaroni, Y. Tobe and S. De Feyter, *Nano Lett.*, 2008, **8**, 2541; (c) J. A. A. W. Elemans, I. De Cat, H. Xu and S. De Feyter, *Chem. Soc. Rev.*, 2009, **38**, 722; (d) T. Chen, W. H. Yang, D. Wang and L. J. Wan, *Nat. Commun.*, 2013, **4**, 1389; (e) S. Yagai, M. Suzuki, X. Lin, M. Gushiken, T. Noguchi, T. Karatsu, A. Kitamura, A. Saeki, S. Seki, Y. Kikkawa, Y. Tani and K. I. Nakayama, *Chem. Eur. J.*, 2014, **20**, 16128.
- (a) S. Lei, K. Tahara, F. C. De Schryver, M. Van der Auweraer, Y. Tobe and S. De Feyter, *Angew. Chem. Int. Ed.*, 2008, **47**, 2964; (b) N. Thi Ngoc Ha, T. G. Gopakumar and M. Hietschold, *J. Phys. Chem. C*, 2011, **115**, 21743; (c) A. Ciesielski, P. J. Szabelski, W. Rzyśko, A. Cadetdu, T. R. Cook, P. J. Stang and P. Samori, *J. Am. Chem. Soc.*, 2013, **135**, 6942; (d) S. Zhang, J. Zhang, K. Deng, J. Xie, W. Duan and Q. Zeng, *Phys. Chem. Chem. Phys.*, 2015, **17**, 24462; (e) L. Xu, X. Miao, L. Cui, P. Liu, K. Miao, X. Chen and W. Deng, *J. Phys. Chem. C*, 2015, **119**, 17920; (f) V. Stepanenko, R. Kandaneli, S. Uemura, F. Würthner and G. Fernández, *Chem. Sci.*, 2015, **6**, 5853. (g) F. Silly, *J. Phys. Chem. C*, 2017, **121**, 10413.

Graphical abstract

A bicomponent blend of linear building blocks leads to intermolecular halogen bonding, resulting in the formation of hexagonal arrays.